

## MiR-196a regulates heme oxygenase-1 by silencing Bach1 in the neonatal mouse lung

Hayato Go,<sup>1,3</sup> Ping La,<sup>1</sup> Fumihiko Namba,<sup>1,5</sup> Masato Ito,<sup>5</sup> Guang Yang,<sup>1</sup> Andrey Brydun,<sup>2</sup> Kazuhiko Igarashi,<sup>2</sup> and Phyllis A. Dennery<sup>1,4</sup>

<sup>1</sup>Department of Neonatology, Children's Hospital of Philadelphia, Philadelphia, Pennsylvania; <sup>2</sup>Department of Biochemistry, Tohoku University Graduate School of Medicine, Sendai, Japan; <sup>3</sup>Department of Pediatrics, Fukushima Medical University School of Medicine, Fukushima, Japan; <sup>4</sup>Department of Pediatrics, University of Pennsylvania School of Medicine, Philadelphia, Pennsylvania and Alpert Medical School at Brown University, Providence, Rhode Island; and <sup>5</sup>Department of Pediatrics, Saitama Medical Center, Saitama, Japan

Submitted 21 December 2015; accepted in final form 18 June 2016

**Go H, La P, Namba F, Ito M, Yang G, Brydun A, Igarashi K, Dennery PA.** MiR-196a regulates heme oxygenase-1 by silencing Bach1 in the neonatal mouse lung. *Am J Physiol Lung Cell Mol Physiol* 311: L400–L411, 2016. First published June 24, 2016; doi:10.1152/ajplung.00428.2015.—In the lung, heme oxygenase-1 (HO-1) is developmentally regulated, with its highest expression in the first days of life. In addition, neonatal mice have limited HO-1 induction in hyperoxia compared with adults. However, few reports have addressed the functional effect of microRNAs (miRNAs) in the regulation of HO-1 in vivo. The aims of the present study were to characterize changes in lung miRNA expression during postnatal development and in response to hyperoxic exposure, and to identify miRNAs that target lung HO-1 gene expression. Neonatal (<12 h old) and adult (2 mo old) mice were exposed to room air or hyperoxia (95% oxygen) for 72 h. TaqMan low-density array rodent miRNA assays were used to calculate miRNA expression changes between control and hyperoxia groups in neonatal and adult lungs. In neonates, we identified miR-196a, which binds to the 3'-untranslated region of the transcriptional repressor BTB and CNC homology 1 (Bach1) and regulates its expression, and subsequently leads to higher levels of lung HO-1 mRNA compared with levels in adults. Despite the increase at baseline, miR-196a was degraded in hyperoxia resulting in limited HO-1 induction in neonatal mice lungs. Furthermore, the developmental differences in lung HO-1 gene expression can be explained in part by the variation in miRNA-196a and its effect on Bach1. This report is the first to show developmental differences in lung miR-196a and its effect on Bach1 and HO-1 expression at baseline and in hyperoxia.

microRNA-196a; Bach1; HO-1; hyperoxic lung injury; lung development

BRONCHOPULMONARY DYSPLASIA (BPD) is a debilitating lung disease in premature infants (17). It has a long-ranging effect on lung function and neurodevelopment not only in childhood but also in later life, and constitutes a major public health problem (3, 5, 37). This condition results from a complex interplay of perinatal factors including maternal inflammation, surfactant deficiency, ventilation, and oxygen toxicity (10).

One important factor in mitigating inflammation and oxidative stress is heme oxygenase (HO), in particular the inducible form, HO-1. In the reaction catalyzed by HO-1, heme is degraded to generate equimolar amounts of biologically active

products, among which biliverdin, an antioxidant, and carbon monoxide, a signaling molecule, are generated. This cytoprotective enzyme is highly expressed in the neonatal lung, perhaps as a defense against perinatal oxidative injury. Paradoxically, in neonatal rats less than 12 h old, despite increased basal levels of lung HO-1 protein, no significant increase was observed after a 3-day exposure to hyperoxia, in contrast to adults with low basal levels but a significant hyperoxic induction (14). This lack of further induction in the neonatal lung may be important in the cytoprotective response because excessively high levels of HO-1 are detrimental (29), whereas more moderate levels are cytoprotective against hyperoxia (35).

HO-1 gene expression is regulated by the transcriptional repressor BTB and CNC homology 1 (Bach1), and the activator nuclear factor-E2-related factor-2 (Nrf2). These two factors compete for binding with small Maf proteins on the antioxidant response element of the HO-1 promoter to suppress or induce its expression, respectively. This is particularly evident in neonatal mice lungs, in which compared with the lungs of adults, increased protein levels and DNA binding of Bach1 are observed after exposure to hyperoxia. This correlates with minimal induction of HO-1 in neonates (9).

Another means of regulating gene expression is via microRNAs (miRNAs). Their discovery has added a new dimension into regulatory mechanisms that control development and disease (4, 40). These are 21- to 24-nucleotide noncoding RNAs targeting to the 3'-untranslated region (UTR) of target genes that repress translation and/or induce degradation of target gene mRNA (33). Accumulated evidence supports the concept that dysregulation of multiple proteins by miRNAs contributes to the pathogenesis of various diseases (12). However, few reports have addressed the functional effect of miRNAs in the regulation of HO-1 in vivo.

We hypothesized that in hyperoxia, changes in miRNA expression during postnatal lung development may contribute to differential HO-1 expression in neonates compared with adults. The aims of the present study were to 1) characterize changes in lung miRNA expression during postnatal development and in response to hyperoxic exposure, and 2) identify miRNAs that target lung HO-1 gene expression. Understanding the mechanisms by which HO-1 is regulated and deciphering whether miRNAs affect its physiologic function may allow for the development of specific therapeutic strategies to maximize the cytoprotective effects of HO-1 and thereby improve tolerance to hyperoxia.

Address for reprint requests and other correspondence: P. A. Dennery, Depts. of Pediatrics and Molecular Biology, Cell Biology and Biochemistry, Warren Alpert Medical School of Brown Univ., 593 Eddy St., Providence, RI 02903 (e-mail: phyllis\_dennery@brown.edu).

Table 1. *Primer sequences for miRNAs*

Assay Name	miRBase ID*	Mature Sequences
hsa-miR-196a	mmu-miR-196a	UAGGUAGUUCUUGUUGUGG
hsa-miR-196b	mmu-miR-196b	UAGGUAGUUCUUGUUGUGG
mmu-miR-146b	mmu-miR-146b	UGAGAACUGAAUCCAUAGGCU
mmu-miR-137	mmu-miR-137	ACGGGUAUUCUUGGGUGGAUAA
mmu-miR-98	mmu-miR-98	UGAGGUAGUAGUUGUUAUUGUU
hsa-miR-27b	mmu-miR-27b	UUCACAGUGGCUAAGUUCUGC
hsa-miR-410	mmu-miR-410	AAUAUAACACAGAUGGCCUGU

\*Version 14.

## MATERIALS AND METHODS

**Mice and hyperoxic exposure.** C57BL/6 wild-type (WT) and Bach1 knockout (KO) mice were housed at Children's Hospital Research Institute Animal Laboratory Facility and Saitama Medical Center Animal Laboratory Faculty. All protocols were reviewed and approved by the Children's Hospital Institutional Animal Care and Use Committee in accordance with the *Guide for the Care and Use of Laboratory Animals* (Bethesda, MD: National Institutes of Health) and Saitama Medical Center Animal Laboratory. Neonatal (<12 h old) and adult mice (2 mo old) were exposed to room air (air) or hyperoxia (95% O<sub>2</sub>) for 72 h. Hyperoxic exposure was conducted in an A-chamber (BioSpherix, Redfield, NY), which allows for continuous monitoring and regulation of O<sub>2</sub> and CO<sub>2</sub>. Ambient carbon dioxide was maintained at <1,500 parts per million by adjusting the chamber's ventilation. For neonatal exposures, pups were cross-nurtured every 24 h by dams that were exposed to room air to obviate hyperoxic injury in the mothers.

**Collection of lung samples.** Lung samples were obtained from neonatal mice exposed to air (control), or hyperoxia for 3 days and from adult mice similarly exposed. After exposure, mice were anesthetized with an intraperitoneal injection of ketamine hydrochloride and xylazine hydrochloride, and the pulmonary artery was perfused with PBS. The right lung was then excised and snap-frozen in liquid nitrogen for further analysis.

**RNA isolation.** RNA was extracted with the mirVana miRNA Isolation kit (Ambion) and used for miRNA and mRNA expression analysis. Total RNA concentration was determined using a NanoDrop 1000 spectrophotometer (Thermo Fisher Scientific), and quality was assessed using Agilent 2100 Bioanalyser (Agilent Technologies). Only the samples meeting the criteria of a 260/230 ratio >1.8 and an RNA integrity number (RIN) ≥7.0 were used.

**Quantitative real-time PCR for mRNA and miRNA.** Steady-state mRNA and miRNA levels were evaluated by quantitative real-time PCR using a TaqMan gene expression system (Applied Biosystems). For mRNA quantitative PCR (qPCR), the first-strand cDNA was synthesized with SuperScript III reverse transcriptase (Invitrogen) and random primers. Gene-specific mRNA levels were determined using TaqMan gene expression assays (each primer at 900 nM and probe at 250 nM; Applied Biosystems) designed over exon-to-exon boundaries. For miRNA qPCR, we used a TaqMan microRNA RT kit (Applied Biosystems) and chose one set of primers and a probe from Applied Biosystems (Table 1). Specific primers for each miRNA are listed in Table 1. All reactions were performed in 384-well plates with a final volume of 10 µl. Real-time PCR plates were analyzed using the Prism 7900HT sequence detection system with Prism SDS2.4 software (Applied Biosystems). Expression analysis was performed in triplicate for each sample. Detection of HO-1 and Bach1 mRNA levels by real-time PCR was performed with the TaqMan gene expression assay (HO-1, Mm 00516004\_m1; Bach1, Mm 01344527\_m1; Nrf2, Mm 0047784\_m1; Applied Biosystems). Relative quantitation was achieved by normalization to the value of small nucleolar RNA 202 (sno202) for miRNA expression and to 18S ribosomal RNA (18S) mRNA for mRNA expression with a TaqMan

gene expression assay (Hs 99999901\_s1; Applied Biosystems) for mRNA expression, using the cycle threshold ( $\Delta\Delta C_t$ ) method.

**MicroRNA array.** TaqMan low-density array (TLDA) rodent miRNA assays (version 2.0; Applied Biosystems) were used to calculate miRNA expression changes between control and hyperoxia groups. For the miRNA array, we pooled 100 ng of total RNA from three samples for each group. Briefly, cDNA was generated using a TaqMan reverse transcription kit and Megaplex primer pools A and B (Applied Biosystems). PCR amplification was carried out using a TaqMan PreAmp Master Mix (Applied Biosystems) and Megaplex PreAmp Pool (Applied Biosystems) containing all the primers for detection by TaqMan gene expression assays for microarray analysis. The lung expression of each miRNA was measured using TaqMan low-density array (TLDA) cards A and B (TLDA rodent miRNA v3.0; Applied Biosystems). PCR was performed on a 7900HT fast-real-time PCR system (Applied Biosystems). Fold changes in expressions of each miRNA were calculated by the  $\Delta\Delta C_t$  method using SDS (version 2.4) and SDS RQ Manager (version 1.2) software.

MicroRNA expression profiling was performed using Expression Suite (Applied Biosystems) software. The analysis setting allowed a maximum  $C_t$  value of 32, and the threshold was 0.2. The data discussed in this publication have been deposited in the Gene Expression Omnibus (GEO) with the National Center for Biotechnology Information (<http://www.ncbi.nlm.nih.gov/geo/>) and are accessible through GEO series accession number GSE70873.

**Target miRNA and mRNA prediction.** MicroRNAs that increased more than twofold compared with those of control animals were defined as being upregulated, and those that decreased more than half compared with control animals were defined as being downregulated. From these, we selected Hmox-1, Bach1-1, Nrf2, Maf, and Kelch-like

Table 2. *Lung miRNAs targeting HO-1 related gene in hyperoxia and during development*

	miRBase ID	Fold Change	Target Gene
Neo (O <sub>2</sub> )/Neo (Air)			
Upregulated	mmu-miR-196b	3.37	Bach1
	mmu-miR-365	2.78	Maf
	mmu-miR-146b	2.77	Bach1
	mmu-miR-137	2.46	Bach1 Maf
	mmu-miR-132	2.05	Maf
Downregulated	mmu-miR-363	0.47	Bach1
	mmu-miR-196a	0.418	Bach1
Adult (O <sub>2</sub> )/Adult (Air)			
Upregulated	mmu-miR-98	3.05	Bach1
	mmu-let-7e	2.96	Bach1
	mmu-miR-23a	2.43	Maf
Neo (Air)/Adult (Air)			
Upregulated	mmu-miR-196a	250	Bach1
	mmu-miR-382	66.7	Bach1
	mmu-miR-410	62.5	Maf
	mmu-miR-135b	58.8	Bach1
	mmu-miR-543	43.3	Maf
	mmu-miR-301a	6	Maf
	mmu-miR-494	5.6	Bach1
	mmu-miR-137	4.2	Maf
	mmu-miR-135a	3.2	Bach1
	mmu-miR-301b	2.8	Maf
	mmu-miR-196b	2.4	Bach1
	mmu-miR-32	2.3	Bach1
	mmu-miR-200b	2.2	Maf
	mmu-miR-98	2.2	Bach1
	mmu-miR-130a	2.1	Maf
	mmu-miR-142-3p	0.47	Bach1
	mmu-miR-27b	0.46	Nfe2l2
	mmu-miR-140	0.45	Bach1
Downregulated	mmu-miR-145	0.38	Maf
	mmu-miR-30d	0.35	Maf

ECH-associated protein 1 (Keap1) as potential Hmox-1-related gene targets. Potential miRNA gene targets were identified using the search engines miRBase (<http://microRNA.sanger.ac.uk>), PicTar ([http://dorina.mdc-berlin.de/rbp\\_browser/dorina.html](http://dorina.mdc-berlin.de/rbp_browser/dorina.html)), and TargetScan version 5.1 (<http://www.targetscan.org/index.html>). A potential gene target was required to be predicted by a minimum of two out of three of these programs, as previously described (24).

**Western blotting.** Protein levels were determined as described (29, 30) and were detected using an enhanced chemiluminescence detection kit (GE Healthcare) after overnight incubation of the membrane with the following antibodies: HO-1 (SPA-896, dilution 1:1,000; Stressgen), Bach1 (A1-5, dilution 1:1,000) (34), calnexin (SPA-860, dilution 1:10,000; Santa Cruz Biotechnology), and Nrf2 (sc-722 dilution 1:500; Santa Cruz Biotechnology), followed by secondary anti-mouse or anti-rabbit horseradish peroxidase-conjugated antibodies (dilution 1:5,000; Santa Cruz Biotechnology). In some experiments, cell lysates were prepared in lysis buffer following 48–72 h of transfection with varying concentrations of miR-196a or control mimic. Western blot analysis was performed as described above.

**Cell culture and hyperoxic exposures.** WT mouse embryonic fibroblast cells (MEFs) and Bach1 KO MEFs were cultured in DMEM containing 10% FBS and 100 units/ml ampicillin (Gibco Life Technologies). To obtain MEFs, WT mice were time-mated. Embryos at *embryonic day 13.5* were collected and minced in PBS. The minced tissue was placed in trypsin/EDTA and incubated at 37°C for 10 min. The suspension was spun at 1,000 revolutions per minute for 5 min at 10°C. NIH3T3 cells stably transfected with a 15-kb oxidant-responsive HO-1 promoter-luciferase construct (HO-1/Luc) were also maintained in DMEM (1). All cells were incubated in a humidified atmosphere of 5% CO<sub>2</sub> at 37°C. The pellet was resuspended in DMEM with 10% FBS, 1% nonessential amino acids, and 1% antibiotic/antimycotic and plated on a cell culture flask. The medium was changed the next day to remove cellular debris. Cells were maintained at subconfluence by passaging every 3 days with 0.05% trypsin-EDTA. MEFs were exposed to hyperoxia (95% O<sub>2</sub>/5% CO<sub>2</sub>) for 24 h in a C-Chamber (BioSpherix, Redfield, NY). Bach1 KO MEFs were a gift from Dr. Kazuhiko Igarashi (Tohoku University Graduate School of Medicine, Sendai, Japan).

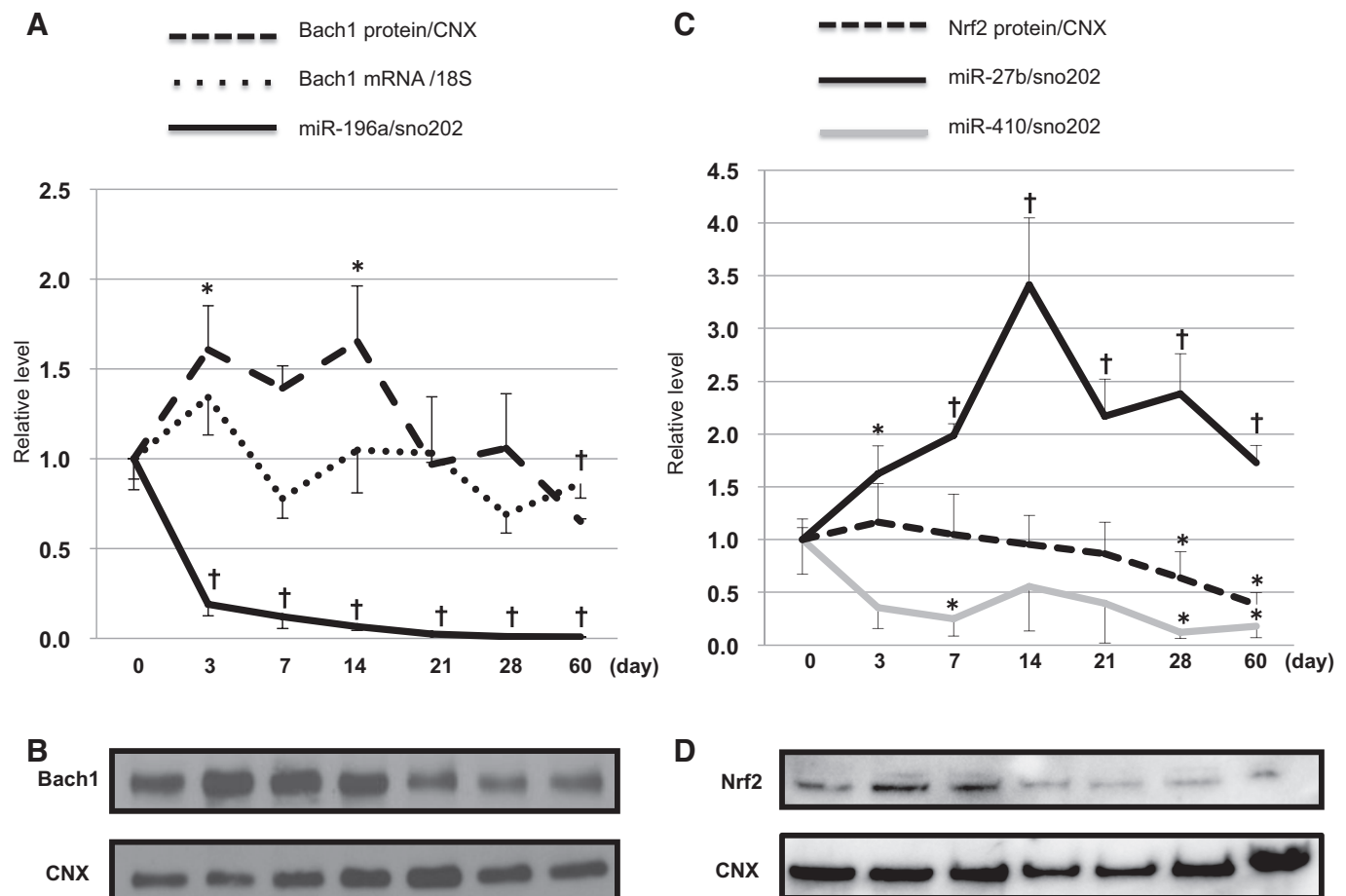


Fig. 1. Developmental expression of microRNA (miR)-196a, miR-27b, miR-410, mRNA of the transcriptional repressor BTB and CNC homology 1 (Bach1), and proteins of Bach1 and the activator nuclear factor-E2-related factor-2 (Nrf2) in the mouse lung. **A**: expression levels of miR-196a, Bach1 mRNA, and Bach1 protein during postnatal lung development were measured by real-time PCR ( $n = 6$ /time point) and Western blot ( $n = 5$ /time point). Levels of miR-196a are normalized to those of small nucleolar RNA 202 (sno202). Bach1 mRNA levels are normalized to those of 18S ribosomal RNA (18S). Values are presented as means  $\pm$  SE. **B**: lungs from wild-type (WT) C57BL/6 mice during lung development were harvested and homogenized with a cocktail of phosphatase and kinase inhibitors. The protein concentration was quantified using the bincinchoninic acid (BCA) method. Equal concentrations were then loaded onto a gel and blotted for Bach1 and calnexin as a loading control. The Western blots shown are the best representatives of five experiments using five different animals in each condition. **C**: expression levels of miR-27b, miR-410, and Nrf2 protein during postnatal lung development were measured by real-time PCR ( $n = 5$ /time point) and Western blot. Values of miR-27b and miR-410 levels are presented as means  $\pm$  SE from five mice. Levels of miR-27b and miR-410 are normalized to those of sno202. **D**: lungs from WT C57BL/6 mice during lung development were harvested and homogenized with a cocktail of phosphatase and kinase inhibitors. The protein concentration was quantified using the BCA method. Equal concentrations were then loaded onto a gel and blotted for Nrf2 and calnexin as a loading control ( $n = 5$ /time point). Data are shown as a relative level normalized to day 0 neonates.  $\dagger P < 0.01$ ;  $*P < 0.05$  vs. day 0 for miR-196a, day 0 for Bach1 protein, day 0 for Nrf2 protein, and day 0 for miR-27b and miR-410.

**Transfection with miRNA mimics and inhibitors.** The mirVana miRNA mimic, negative control, and inhibitors of miR-196a were obtained from Ambion. MEFs or HO-1/Luc cells were transfected with 10–30 nM of miRNA mimics or 5 or 10 nM inhibitors using Lipofectamine 2000 or Lipofectamine RNAi Max (Invitrogen) according to the manufacturer's protocol. After 48–72 h of transfection, cells were then harvested for assays.

**Plasmids.** The Bach1 3'-UTR was first PCR-amplified from reverse transcription products of total murine mRNA. To generate a luciferase Bach1 3'-UTR construct, Renilla luciferase gene in pRL-TK plasmid (Promega) was replaced with humanized firefly luciferase, termed pRLUC-TK. To generate pRLUC-TK-Bach1 3'-UTR mice, the Bach1 3'-UTR was PCR-amplified and replaced by an SV40 late poly(A) site in pRLUC-TK.

**Luciferase reporter assay.** MEFs were seeded in 6- or 12-well plates 1 day before transfection with pGL3-Bach1-UTR, miR-196a mimic, or inhibitor using Lipofectamine 2000 (Invitrogen). A scrambled sequence was used as a negative control. HO-1/Luc cells were also seeded in a 12-well plate 1 day before transfection with miR-196a mimic, inhibitor, or negative control. MEFs and HO-1/Luc cells were collected 48 and/or 72 h after transfection, and relative luciferase intensity was measured using an In Vivo Imaging System (IVIS;

Xenogen, San Francisco, CA) as previously described (46). The photons were normalized to cell numbers.

**Statistical analysis.** All data are presented as means  $\pm$  SE of separate experiments. For comparison between treatment groups, the null hypothesis that there is no difference between treatment means that it was tested with a Student's *t*-test for two groups and one-way ANOVA for multiple groups and linear regression. Statistical significance was considered at  $P < 0.05$ .

## RESULTS

**miR-196a, mir-27b, and mir-410 levels are changed during lung development.** During postnatal lung development, 50 miRNAs increased, and 151 miRNAs decreased by more than twofold (data not shown). Out of those miRNAs, 20 miRNAs related to Bach1, Nrf2, and Maf were altered (Table 2), however, no miRNAs that directly regulate HO-1 were found. Several miRNAs with Bach1 as a direct target were identified. MiR-196a had the highest fold change among those miRNAs. In contrast, only one miRNA with Nrf2 as a direct target, miR-27b, was identified in the array data and was significantly

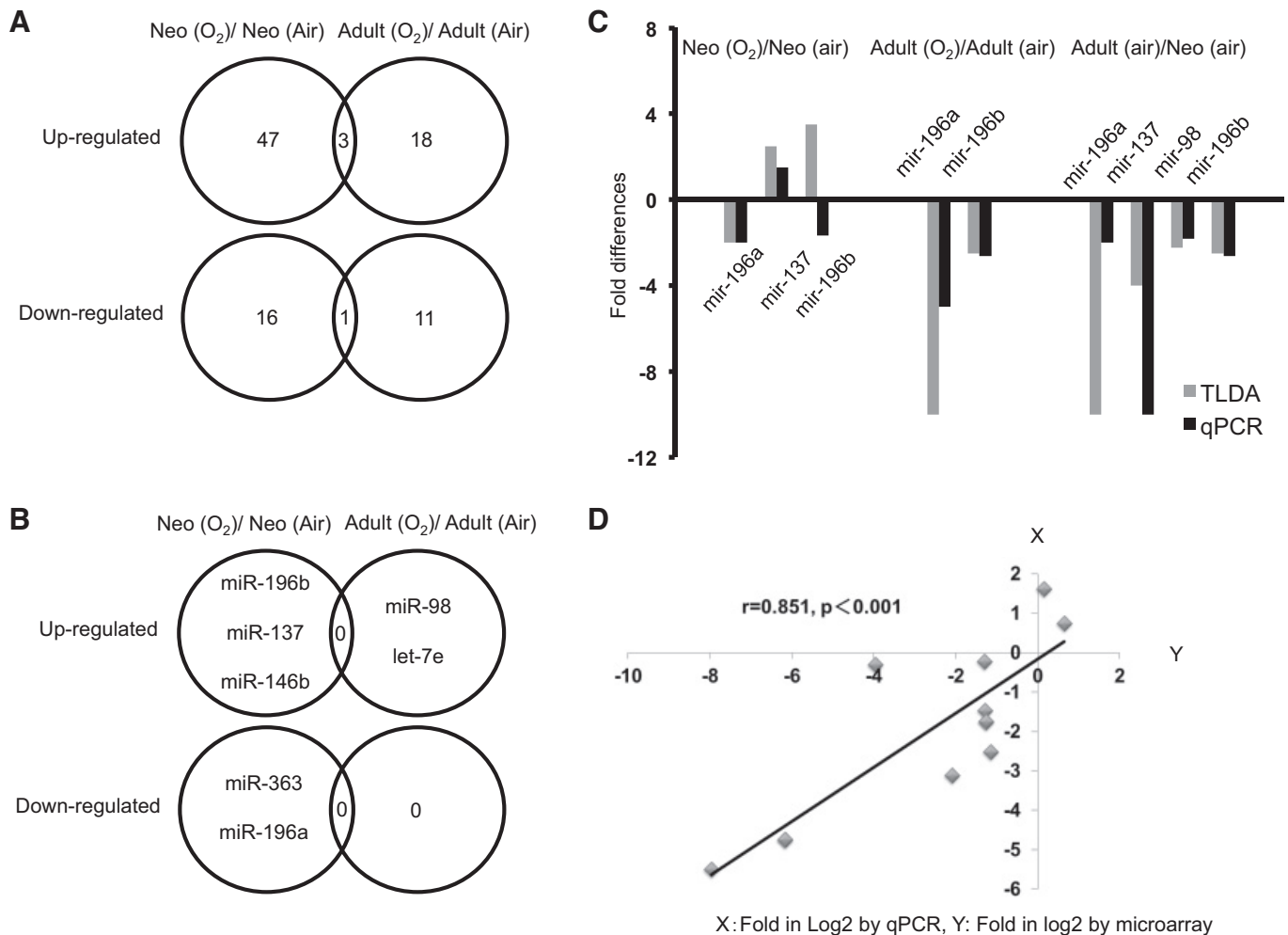


Fig. 2. Altered miRNAs in neonatal vs. adult mouse lung. A: Venn diagram of altered miRNAs in neonatal vs. adult lungs. Fifty miRNAs increased more than twofold, and 17 miRNAs decreased by more than half in neonates exposed to hyperoxia. In adults exposed to hyperoxia, 21 miRNAs increased more than twofold, and 12 miRNAs decreased by more than half. B: this Venn diagram of miRNA related to Bach1 shows no altered miRNAs common to either neonatal or adult lungs exposed to hyperoxia on the basis of array data. C: selected miRNAs from the miRNA expression profile were validated by RT-quantitative PCR (qPCR). D: correlation between data from microarray and RT-PCR for selected miRNAs was performed using linear regression. The x-axis represents fold in log<sub>2</sub> by qPCR; the y-axis represents fold in log<sub>2</sub> by TaqMan low-density array data.



downregulated in neonates compared with adults. We also selected miR-410 as another known Nrf2-targeted miRNA (25). To further verify maturational differences in HO-1 regulation, we measured miR-196a and Bach1 expression as well as miR-27b, miR-410, and Nrf2 expression during postnatal lung development. During the early postnatal period, miR-196a was significantly decreased and Bach1 protein levels were significantly increased (Fig. 1, A and B), whereas miR-27b levels were increased and miR-410 levels were decreased with advanced postnatal age. Interestingly, Nrf2 protein mirrored the expression of miR-27b and was inversely correlated with miR-410 during early postnatal age (Fig. 1, C and D), which would suggest that miR-410, rather than miR-27b, regulates Nrf2 during early postnatal age.

**Hyperoxic exposure alters lung miRNAs in neonates and adults.** After hyperoxic exposure, out of the miRNAs we examined, 50 miRNAs were increased and 17 miRNAs were decreased in neonates, whereas 21 miRNAs were increased and 12 miRNAs were decreased by more than twofold in adults (Fig. 2A). As shown in Table 2, many miRNAs related to Bach1 and Maf were altered in hyperoxia, however, no miRNAs that directly regulate HO-1 were found. As shown in Figure 1B, none of the altered miRNAs with Bach1 as a direct target were common to either neonatal or adult lungs exposed to hyperoxia, suggesting important maturational differences in miRNA expression. In neonatal lungs, lung miR-196b, miR-137, and miR-146b were upregulated, whereas miR-363 and miR-196a were downregulated after hyperoxia (Fig. 2B). In adult lungs after hyperoxia, miR-98 and let-7e, which have Bach1 as a potential gene target, were upregulated, but no miRNAs were downregulated (Fig. 2B). We verified that there was good correlation between microarray and RT-PCR data (Fig. 2, C and D).

**Lung miR-196a, Bach1, and HO-1 are differentially regulated in neonates and adults exposed to hyperoxia.** Because we had previously shown that Bach1 plays an important role in the regulation of HO-1 in neonates exposed to hyperoxia (9), we were particularly interested in miR-196a, which has Bach1 as a potential target and was upregulated 250-fold in neonates compared with adults and downregulated in neonates after hyperoxia (Table 2, Fig. 3A).

It is known that there are clear differences in HO-1 gene regulation between neonatal and adult lungs exposed to

hyperoxia. As we previously documented (9), lung HO-1 mRNA was increased in both neonates and adults after hyperoxia (Fig. 3B).

Bach1 mRNA levels were not changed in either neonatal or adult lungs exposed to hyperoxia (Fig. 3C). However, Bach1 protein levels were significantly altered in neonatal lungs exposed to hyperoxia compared with air, whereas there were no changes in adults (Fig. 3D). This documents the differential importance of Bach1 in the regulation of HO-1 during postnatal lung development.

**Hyperoxia alters miR-196a and Bach1 in MEFs.** We also verified changes in Bach1 binding to the 3'-UTR, and Bach1 mRNA protein and HO-1 mRNA levels after hyperoxia in MEFs (Fig. 4). After 4 h of hyperoxic exposure, relative light intensity was significantly increased and peaked at 24 h of hyperoxia (Fig. 4A). In agreement with the *in vivo* results, miR-196a levels were downregulated in MEFs exposed to hyperoxia (Fig. 4B). In addition, Bach1 protein (Fig. 4C) and HO-1 mRNA (Fig. 4D) levels increased after 24 h of hyperoxia, but no changes in Bach1 mRNA levels were observed (Fig. 4E). This validated the *in vivo* observations and confirmed that MEFs could serve as a model in our study.

**MiR-196a regulates Bach1 and HO-1 in MEFs.** We then evaluated the mechanisms by which miR-196a altered Bach1 using a 3'-UTR reporter assay to confirm whether miR-196a binds the 3'-UTR of the Bach1 gene. The 3'-UTR region of Bach1 (WT) was cloned at the binding site into a pRL-TK vector containing Renilla luciferase, and relative light intensity after transfection was compared in transfected MEFs exposed to room air/5% CO<sub>2</sub> and hyperoxia (95% O<sub>2</sub>/5% CO<sub>2</sub>). Cotransfection of the negative control and the Bach1 3'-UTR plasmid did not change the relative light intensity (Fig. 5A). Cotransfection of an miR-196a mimic and the Bach1 3'-UTR plasmid decreased relative light intensity (Fig. 5B), whereas cotransfection of an miR-196a inhibitor and the Bach1 3'-UTR plasmid increased relative light intensity (Fig. 5C). These data demonstrate that miR-196a directly binds to the 3'-UTR of Bach1. To further verify that Bach1 was the target of miR-196a, we transfected the MEFs with an miR-196a mimic or inhibitor and evaluated Bach1 mRNA and protein levels. We confirmed that miR-196a levels were increased after transfection of the miR-196a mimic and decreased after transfection of the miR-196a inhibitor (Fig. 5D). Although Bach1 mRNA

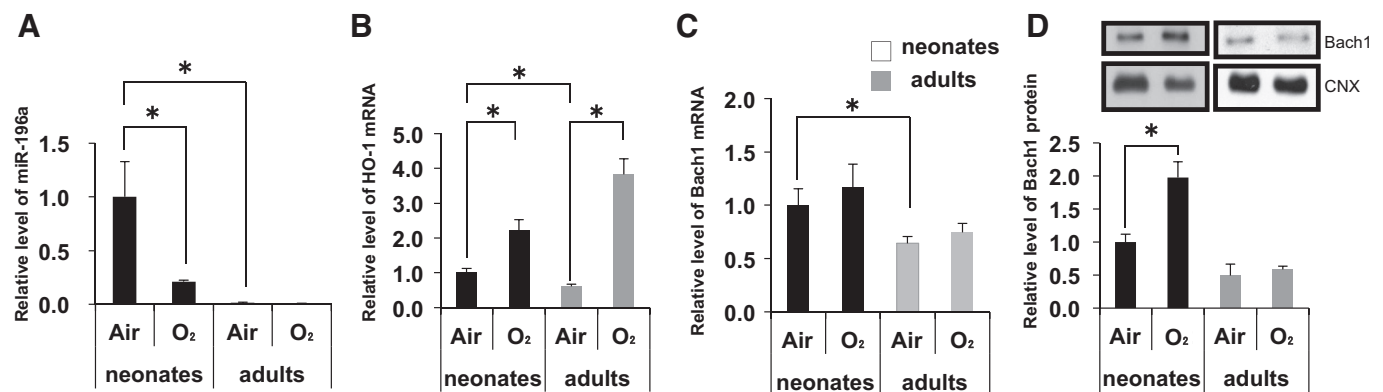


Fig. 3. Differential regulation of lung miR-196a, Bach-1, and heme oxygenase-1 (HO-1) in neonate and adult mice exposed to hyperoxia. A–C: miR-196a, HO-1 mRNA, and Bach1 mRNA levels, respectively, in neonatal and adult lungs exposed to hyperoxia. Values are presented as means  $\pm$  SE of six separate determinations. D: Bach1 protein level in neonatal and adult lungs exposed to hyperoxia. Calnexin (CNX) is shown as a loading control. Densitometric evaluation of protein expression normalized to calnexin is provided. Values are presented as means  $\pm$  SE of four separate determinations; \* $P$  < 0.05 vs. air.

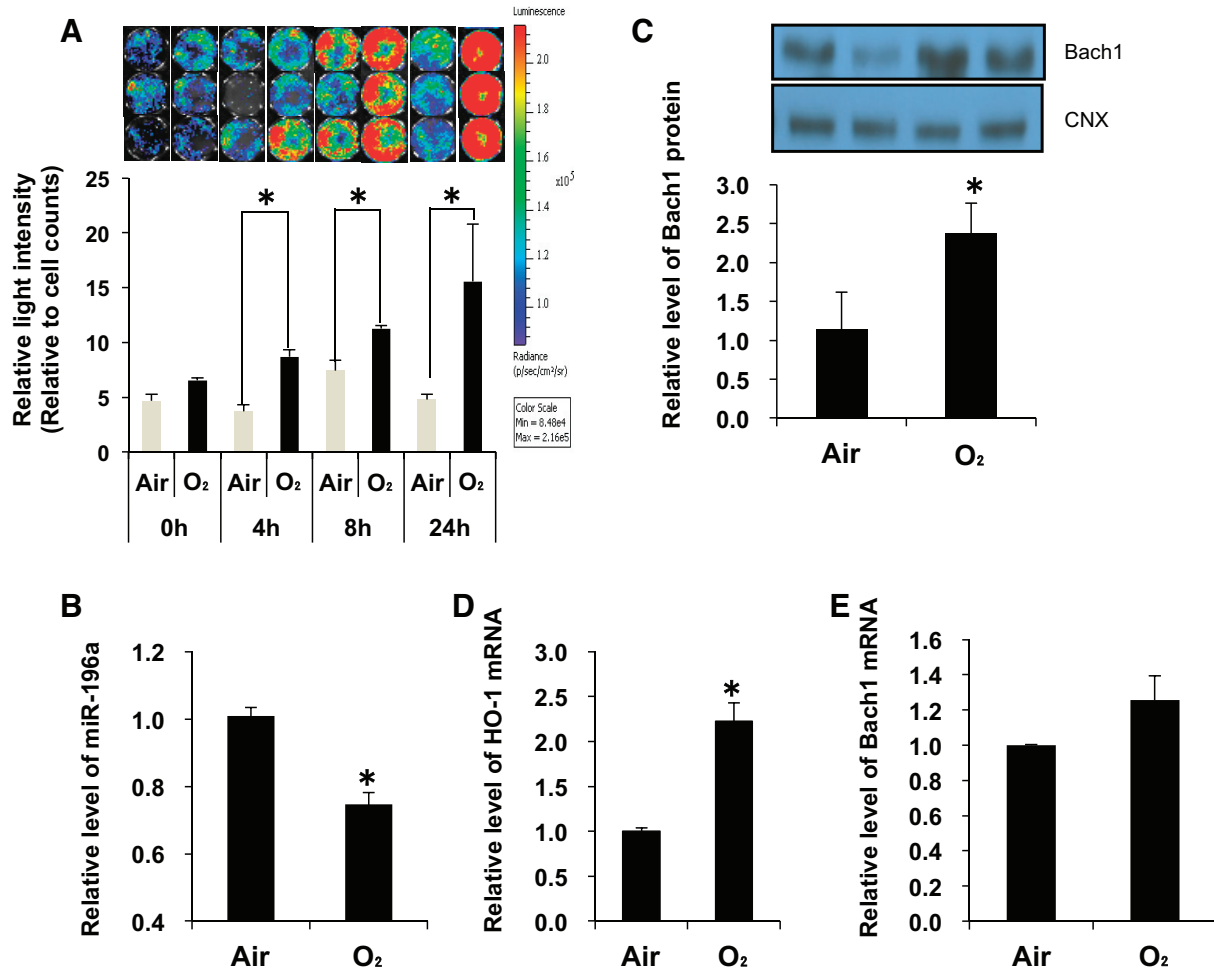


Fig. 4. Hyperoxia alters miR-196a and Bach-1 in mouse embryonic fibroblast cells (MEFs). **A:** luciferase activity after hyperoxia in MEFs. Twenty-four hours after transfection of the Bach1 3'-untranslated region (UTR) plasmid, MEFs were exposed to hyperoxia. Relative light intensity was measured 4, 8, and 24 h after hyperoxia. The color scale bar represents photon emission intensity. Values are presented as means  $\pm$  SE of six separate determinations; \* $P$  < 0.05. **B:** miR-196a levels were measured by qPCR. Levels of miR-196a are normalized to those of sno202. **C:** Bach1 protein levels were measured by Western blot [calnexin (CNX) is shown as a loading control], and densitometric evaluation of protein expression normalized to loading control (CNX). **D** and **E:** HO-1 mRNA and Bach1 mRNA levels were measured by qPCR. Levels of miR-196a are normalized to those of sno202; HO-1 and Bach1 mRNA levels are normalized to those of 18S. Values are presented as means  $\pm$  SE of four separate determinations; \* $P$  < 0.05.

levels were not changed after transfection of miR-196a mimic and/or inhibitor compared with mock transfection (Fig. 5E) (mock transfection represents mice treated with Lipofectamine alone), the miR-196a mimic suppressed protein levels of Bach1 (Fig. 5F), whereas the inhibitor resulted in increased protein Bach1 levels (Fig. 5G), indicating that miR-196a indeed targets Bach1 and regulates its endogenous expression in MEF cells. Furthermore, miR-196a mimic upregulated HO-1 mRNA expression and miR-196a inhibitor downregulated HO-1 mRNA via Bach1 (Fig. 5H).

**MiR-196a regulates HO-1 mRNA.** To confirm the regulation of HO-1 mRNA expression by miR-196a, we measured the changes in HO-1 promoter activity in HO-1/Luc 3T3 cells exposed to hyperoxia or air after transfection with negative control, miR-196a mimic, and inhibitor (Fig. 6). After 48 h of transfection, miR-196a mimic and inhibitor did not change luciferase reporter activity when compared with mock transfection (Fig. 6A). However, after a 72-h transfection, the miR-196a inhibitor significantly decreased luciferase reporter

activity and the miR-196a mimic significantly increased luciferase reporter activity when compared with mock transfection (Fig. 6B).

**MiR-196a does not alter HO-1 in Bach1 KO MEFs.** To confirm that miR-196a regulation of HO-1 required Bach1, HO-1 mRNA and protein levels were determined in Bach1 KO MEFs (Fig. 7). Interestingly, HO-1 mRNA and protein levels were not changed in Bach1 KO cells after transfection with miR-196a mimic or inhibitor (Fig. 7, B and D).

**Hyperoxia alters miR-196a and HO-1 mRNA levels in Bach1 KO MEFs and Bach1 KO mouse lung.** In contrast, as shown in Figure 8, lung HO-1 mRNA levels were higher in both neonatal and adult Bach1 KO mice compared with WT mice (Fig. 8A), and the response to hyperoxia was much stronger in adults (Fig. 8B). However, lung miR-196a levels were increased in neonatal Bach1 KO mice, whereas they were unchanged in adult KO mice (Fig. 8C), again suggesting a developmental difference in the regulation of miR-196a. These data also revealed a novel role for Bach1 in the in vivo regulation of

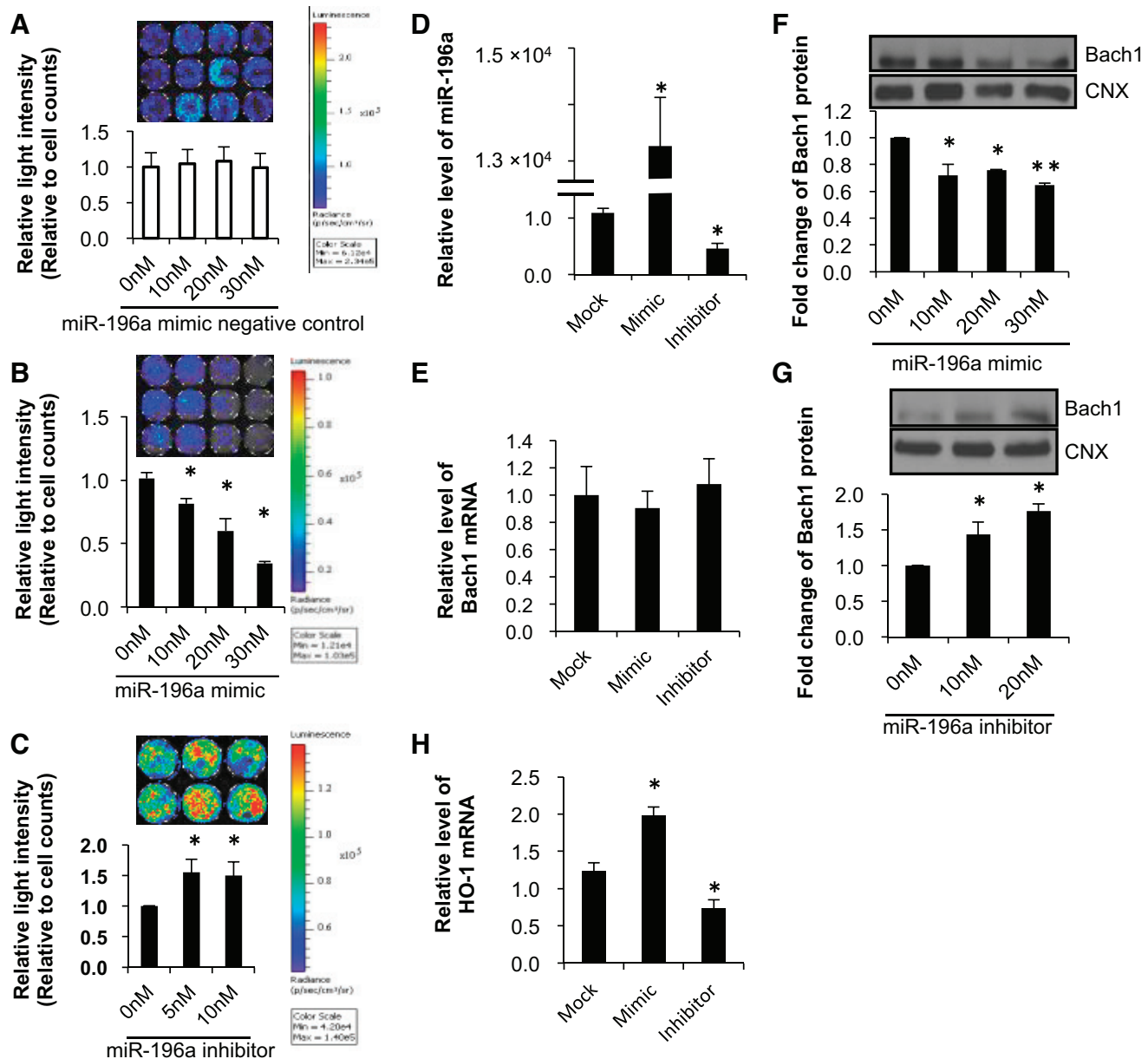


Fig. 5. MicroRNA-196a regulates Bach1 and HO-1 expression. A–C: luciferase activity was determined by measuring photon emission after incubation with the substrate luciferin for 24 h after transfection of Bach1 3'-UTR plasmid and miR-196a control, mimics, and inhibitor. Values for cells with control transfection are set equal to 1. Data are presented as means  $\pm$  SE of six to eight separate determinations. D and E: effect of miR-196a mimic (30 nM) or miR-196a inhibitor (10 nM) on miR-196a and Bach1 levels. MEFs were transfected with miRNA-196a mimics and inhibitor with Lipofectamine 2000 for 72 h. miR-196a levels and Bach1 mRNA levels were measured by qPCR and compared with mock transfection (mock transfection represents mice treated with Lipofectamine alone). Levels of miR-196a are normalized to those of sno202. Bach1 mRNA levels are normalized to those of 18S. Values are presented as means  $\pm$  SE of three separate determinations; \* $P$  < 0.05 vs. mock transfection. F and G: Bach1 protein levels after transfection with miR-196a mimic and inhibitor were measured by Western blot. Calnexin is shown as a loading control. Densitometric evaluation of protein expression normalized to loading control (calnexin; CNX) is provided. Values are presented as means  $\pm$  SE of three separate determinations; \* $P$  < 0.05 vs. 0 nM, \*\* $P$  < 0.001 vs. 0 nM. H: effect of miR-196a mimic (30 nM) or miR-196a inhibitor (10 nM) on HO-1 mRNA levels. MEFs were transfected with miRNA-196a mimics and inhibitor with Lipofectamine 2000 for 72 h. HO-1 mRNA levels were measured by qPCR and compared with mock transfection. HO-1 mRNA levels are normalized to those of 18S. Values are presented as means  $\pm$  SE of three separate determinations; \* $P$  < 0.05 vs. mock transfection.

miR-196a in hyperoxia. Nevertheless, this regulatory effect was not observed in vitro with the Bach1 KO MEFs (Fig. 8D).

## DISCUSSION

Our study is the first to document that miRNAs play an important role in HO-1 regulation during postnatal lung development and in the blunted response of the neonates to oxidative

stress. Expression profiling of miRNAs has provided important new insights into the pathogenesis, classification, diagnosis, and prognosis of many human diseases including lung disease (2, 13, 18, 21, 26, 27, 32, 42, 45). In particular, such approaches have been successfully applied previously in rodent models of BPD (7, 16), revealing that several miRNAs are important contributors to the progression of BPD.

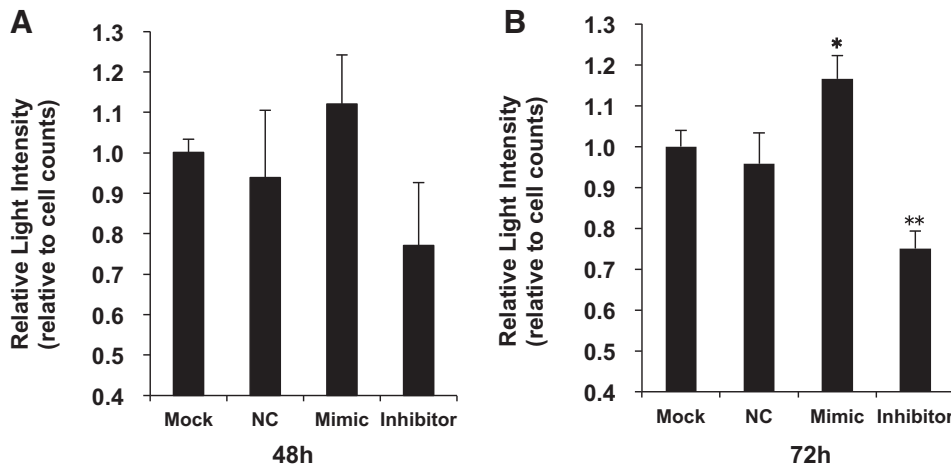


Fig. 6. Relative light intensity in HO-1/Luc cells after transfection of miR-196a mimic and inhibitor. Relative light intensity in HO-1/Luc cells 48 ( $n = 3$ ) (A) and 72 h ( $n = 5$ ) (B) after transfection with negative control (NC), miR-196a mimic, and miR-196a inhibitor. Values were compared with those for mock transfection. This experiment was carried out in normoxia. Values are presented as means  $\pm$  SE of three or five separate determinations; \* $P < 0.05$  vs. mock transfection, \*\* $P < 0.001$  vs. mock transfection.

In terms of the relationship between miRNAs and lung development, a previous study using Dicer-null mice suggested that miRNAs play an important role in embryonic lung morphogenesis (20). Previous reports have demonstrated that expression of miRNAs varies in BLAB mice or during lung

development in Sprague-Dawley rats (28, 41, 44). Additionally, a previous study suggests that several miRNAs, including miR-154, miR-29a, miR-29b, and miR-335 were changed in BALB mice and humans during postnatal lung development (43). The role of miR-196a in lung development had not

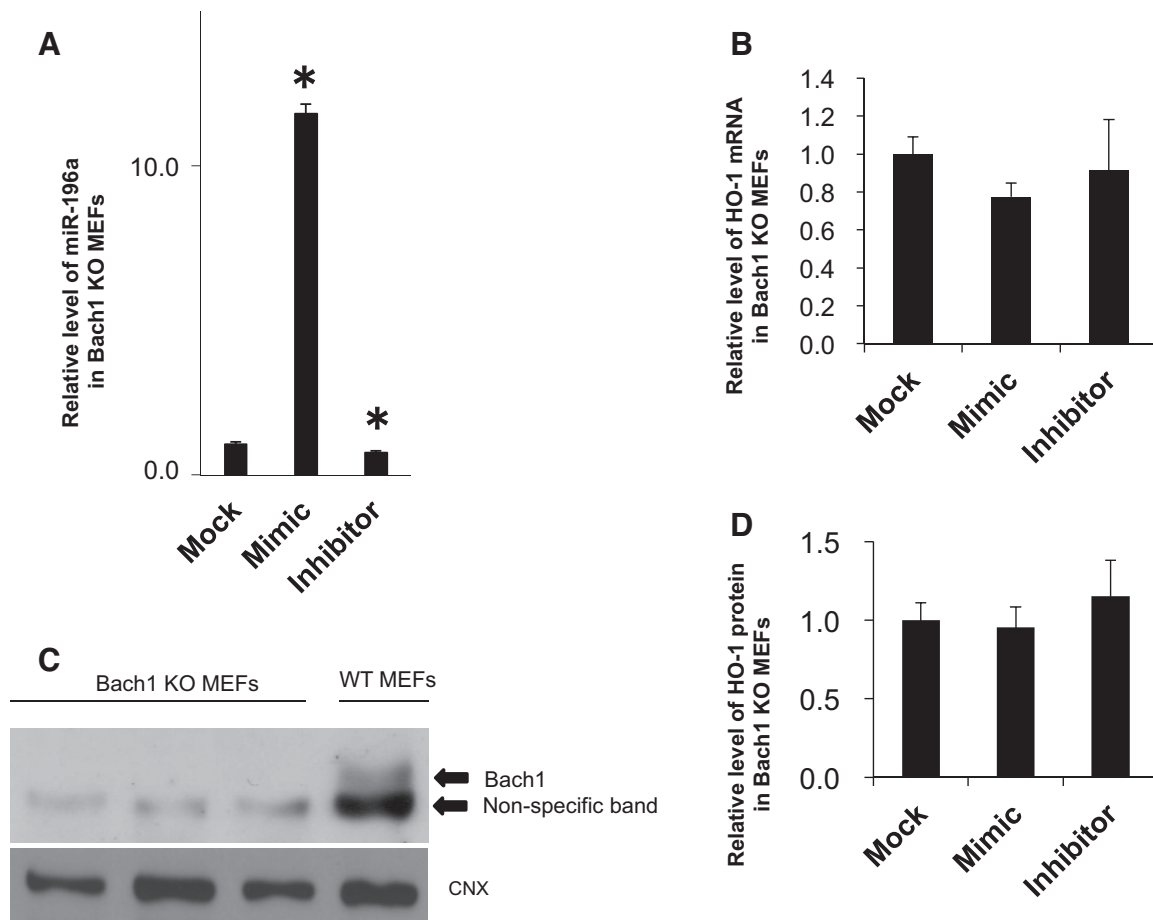


Fig. 7. miR-196a and HO-1 expression after transfection of miR-196a mimic and inhibitor in Bach1 KO MEFs. A: miR-196a levels after transfection of miR-196a mimic and inhibitor. Values are presented as means  $\pm$  SE ( $n = 3$ ); \* $P < 0.05$  vs. mock transfection. B: HO-1 mRNA levels after transfection of miR-196a mimic and inhibitor. Levels of miR-196a are normalized to those of sno202, HO-1 mRNA levels are normalized to those of 18S. Values are presented as means  $\pm$  SE ( $n = 3$ ); \* $P < 0.05$  vs. mock transfection. C and D: Western blots and analysis of Bach1 in Bach1 KO and WT MEFs and HO-1 protein after transfection of miR-196a mimic and inhibitor. HO-1 protein levels are normalized to those of calnexin. Values are presented as means  $\pm$  SE ( $n = 3$ ); \* $P < 0.05$  vs. mock transfection.



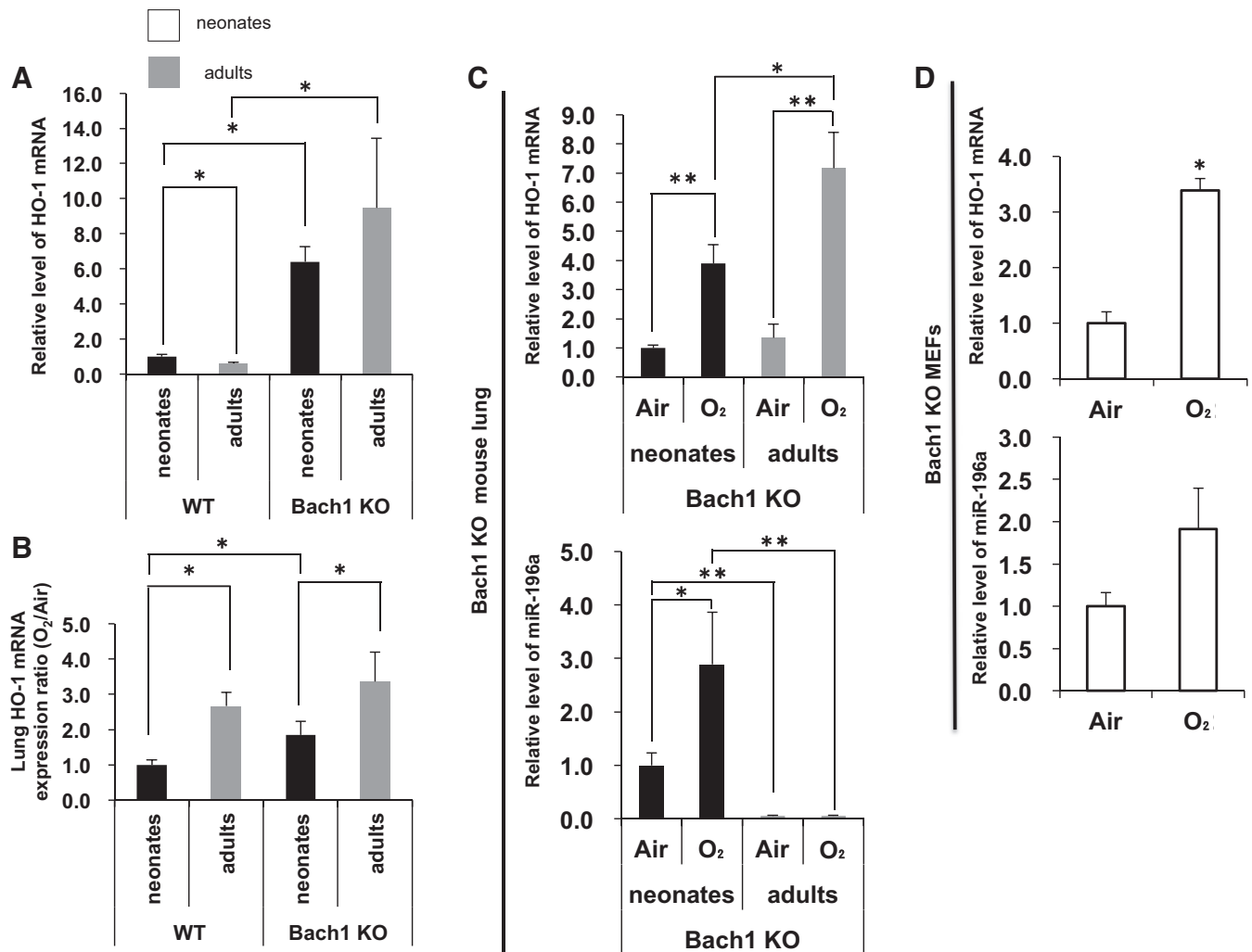


Fig. 8. Hyperoxia alters miR-196a and HO-1 mRNA levels in Bach1 KO MEFs and Bach1 KO mouse lung. A: HO-1 mRNA levels in WT and Bach1 KO mouse lung of neonate and adult mice exposed to air. B: HO-1 inducibility in WT and Bach1 KO mouse lung of neonates and adults exposed to hyperoxia. C: HO-1 mRNA and miR-196a levels in Bach1 KO mouse lung of neonates and adults exposed to hyperoxia. D: HO-1 and miR-196a levels in Bach1 KO MEFs exposed to hyperoxia. The levels of miR-196a are normalized to those of sno202, HO-1 mRNA levels are normalized to those of 18S. Values are presented as means  $\pm$  SE of six (A–C) or three (D) separate determinations; \* $P$  < 0.05 vs. air, \*\* $P$  < 0.01 vs. air.

previously been explored. In our model, we clearly show that this miRNA is key to regulating HO-1 by elevating levels of Bach1, an inhibitor of HO-1 gene expression. Typically, levels of Bach1 are reduced by high levels of heme that promote its degradation and favor the binding of Nrf2 to the antioxidant response element of HO-1 in cooperation with small Maf proteins (34). In this model, we did not evaluate heme levels in neonatal lungs because this would be complicated by hemorrhage in the tissues with dissection and/or injury (hyperoxia). It is therefore not clear whether this is also important in regulating the expression of Bach1 and whether this involves miR-196a.

In our target miRNA prediction, only miR-377 was a candidate that can bind directly to the 3'-UTR of HO-1. A previous study suggested that the combination of miR-377 and miR-217 directly regulates HO-1 protein expression in the presence of hemin in vitro (6). In the current study, we could not detect miR-377 in either neonatal or adult mice lung samples. Nevertheless, several miRNAs related to Bach1 were differentially regulated in neonatal and adult lungs. In our

study, out of miRNAs that were changed during postnatal lung development, our study showed that miR-196a was one of the most important miRNAs that regulate HO-1 mRNA by increasing Bach1 protein in the early postnatal lung.

In the early postnatal period, miR-196a is significantly decreased and Bach1 protein levels are significantly increased, whereas miR-196a levels are lowest in adult lungs compared with those of neonates. Furthermore, we demonstrated both in vivo and in vitro, that miR-196a binds to the 3'-UTR of Bach1 and directly regulates Bach1 protein at the posttranslational level, thereby modulating HO-1 mRNA, as previously described using hepatocytes (23). We have previously shown that nuclear Bach1 protein levels are very low in adult lungs (9). In this study, after *postnatal day 14*, whole lung Bach1 protein levels were also decreased. Although we expected that Bach1 protein levels would be correlated with miR-196a levels during postnatal lung development, we were surprised to see that Bach1 levels were not correlated with miR-196a levels after *postnatal day 14*, implying that in the adult lung, Bach1 is regulated by other miRNAs or by other mechanisms. In fact,

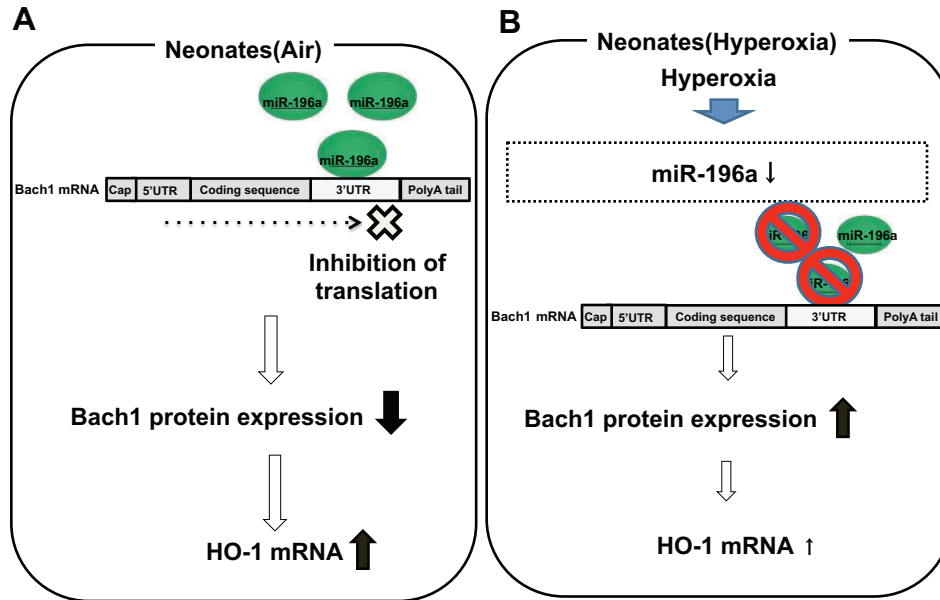


Fig. 9. Schematic representation of the regulation of miR-196a on HO-1 expression via Bach1 in neonatal lungs. A: at birth, miR-196a basal levels in neonatal mouse lung are higher than those of adults. Overexpression of miR-196a increases HO-1 expression via suppressing Bach1. B: in hyperoxia, miR-196a is decreased and Bach1 protein expression is increased, which lessens HO-1 inducibility.

other miRNAs that regulate Bach1, including miR-140 and miR142-3p, were upregulated in adult lungs (Table 2). Their importance in adults needs to be further explored.

We have previously reported that HO-1 mRNA expression in rodents is much higher in the neonatal period than in adults (9, 15, 29). The present study confirms this as well. In our study, despite relatively high levels of Nrf2 in the neonates, Bach1 appears more important in the developmental regulation of lung HO-1. A previous study showed that miR-27b blocks D4/Notch interactions and that in liver development, Notch could induce Nrf2 synthesis (8, 39). We speculate that miR-27b directly regulates Nrf2 expression. In this study, there was a positive rather than a negative correlation between miR-27b and Nrf2 expression during early postnatal lung development. However, after *postnatal day 28*, there was a negative correlation between miR-27b and Nrf2 expression. In contrast, miR-374a, miR-28, miR-708, miR-27b, miR-23a, miR-340, miR-153, miR-507, miR-129, miR-93, miR-144, miR-410, miR-140, miR-129, miR-132, and miR-212 were predicted to bind to the 3'-UTR of Nrf2 (25). Even though we did not identify miR-410 as an miRNA that binds to the 3'-UTR of Nrf2 using our criteria, neonatal lung miR-410 levels were significantly increased in neonates compared with those in adults (Table 2). Therefore, we performed qPCR of miR-410 during lung development. Levels of miR-410 were inversely correlated with Nrf2 expression during the early postnatal period in this study (Fig. 2C). This suggests that miR-410 is one of the miRNAs regulated by Nrf2 in the early postnatal period. Whether miR-27b or miR-410 regulates Nrf2 from *postnatal day 7* to *postnatal day 14* requires further study.

In contrast to its relative abundance in air-exposed neonates, miR-196a is downregulated in neonatal lungs with hyperoxic exposure. This would lead to upregulation of Bach1 protein and reduced inducibility of HO-1 mRNA, as shown in the schematic representation in Figure 9, despite the inductive role of Nrf2. In adults, lung miR-196a is in very low abundance and therefore not likely to have much influence on the regulation of HO-1 at baseline or in hyperoxia. In accordance, as shown in

our study, Bach1 is not as important in the hyperoxic regulation of HO-1 in adults. In fact, when Bach1 is disrupted, regulation of HO-1 in neonates approximates that of adults in hyperoxia, further documenting the importance of Bach1 specifically in neonates when it serves to dampen HO-1 induction.

Interestingly, we uncovered that Bach1 can also negatively regulate miR-196a because Bach1 KO mice and MEFs have increased miR-196a levels compared with those of WT mice.

In this paper, lung miR-98 and let-7e, which can bind to the Bach1 3'-UTR, were also upregulated only in adult mice after hyperoxia. A recent study demonstrates that Huh-7 cells transfected with miR-98 mimic and let-7 families showed increased resistance against oxidant injury (22). We suspect that miR-98 and let-7e play important roles in the regulation of Bach1 gene expression in adult lungs.

Other miRNA candidates binding to the Bach1 3'-UTR, including miR-196b, miR-137, miR-146b, and miR-363 were changed in neonatal lungs after hyperoxia. As in the current study, lung miR-146b was upregulated in a mouse model of acute and chronic asthma (19). This miRNA is known to be associated with inflammatory (11) and innate immune response (31, 36), and is important in the regulation of transforming growth factor- $\beta$  signaling via SMAD4 (38).

Our study has some limitations. We used a mouse model of aseptic BPD (i.e., only hyperoxic exposure). BPD can be caused by other factors including bacterial infection and ventilation, which are known to induce miRNAs in mice (38).

We also investigated only the effects of the miR-196a mimic or inhibitor on Bach1, HO-1, and miR-196a in MEF cells. These cells are not lung cell lines and may have different responses than lung epithelial cells and lung fibroblasts. Finally, we did not evaluate the distribution of miR-196a in neonatal and adult lungs using *in situ* hybridization. This would allow the identification of which cells express miR-196a.

In summary, we demonstrate that the neonatal lungs of mice have high levels of miR-196a compared with the lungs of adults, which results in reduced Bach1 expression and leads to

high levels of HO-1 during development. After hyperoxic exposure, miR-196a is downregulated in neonate mice, which results in upregulation of Bach1 and subsequent relative downregulation of HO-1, in contrast to adults, in which miR-196a does not play a role in HO-1 regulation. Therefore, miR-196a is key to the regulation of HO-1 via Bach1 during postnatal lung development, whereas Nrf2 plays a dominant role in the regulation of HO-1 during hyperoxic exposure. The mechanism by which the expression of miR-196a is regulated during postnatal development and in hyperoxia remains to be further elucidated. We speculate that miR-196a represents a therapeutic target for the regulation of HO-1 in neonates to obviate lung oxidative injury.

## ACKNOWLEDGMENTS

We thank Patrick Fernando and Shaon Sengputa for productive discussions and comments on the manuscript and for their technical help.

## GRANTS

This work was supported by National Institute of Diabetes and Digestive and Kidney Diseases Grant RO1 HL-058752 and by the Warren Alpert Foundation Funds from Brown University, both to P.A. Dennery.

## DISCLOSURES

No conflicts of interest, financial or otherwise, are declared by the authors.

## AUTHOR CONTRIBUTIONS

H.G., G.Y., and P.A.D. conception and design of research; H.G., P.L., F.N., and M.I. performed experiments; H.G., P.L., F.N., and M.I. analyzed data; H.G., F.N., A.B., and K.I. interpreted results of experiments; H.G. prepared figures; H.G. drafted manuscript; H.G., G.Y., and P.A.D. edited and revised manuscript; H.G., P.L., F.N., M.I., G.Y., A.B., K.I., and P.A.D. approved final version of manuscript.

## REFERENCES

- Abate A, Yang G, Wong RJ, Schroder H, Stevenson DK, Dennery PA. Apigenin decreases hemin-mediated heme oxygenase-1 induction. *Free Radic Biol Med* 15: 711–718, 2005.
- Alevizos I, Alexander S, Turner RJ, Illei GG. MicroRNA expression profiles as biomarkers of minor salivary gland inflammation and dysfunction in Sjögren's syndrome. *Arthritis Rheum* 63: 535–544, 2011.
- Baraldi E, Filippone M. Chronic lung disease after premature birth. *N Engl J Med* 357: 1946–1955, 2007.
- Bartel DP. MicroRNAs: genomics, biogenesis, mechanism, function. *Cell* 116: 281–297, 2004.
- Bassler D, Stoll BJ, Schmidt B, Asztalos EV, Roberts RS, Robertson CM, Sauve RS. Using a count of neonatal morbidities to predict poor outcome in extremely low birth weight infants: added role of neonatal infection. *Pediatrics* 123: 313–318, 2009.
- Beckman JD, Chen C, Nguyen J, Thayanithy V, Subramanian S, Steer CJ, Vercellotti GM. Regulation of heme oxygenase-1 protein expression by miR-377 in combination with miR-217. *J Biol Chem* 286: 3194–3202, 2011.
- Bhaskaran M, Xi D, Wang Y, Huang C, Narasaraaju T, Shu W, Zhao C, Xiao X, More S, Breshears M, Liu L. Identification of microRNAs changed in the neonatal lungs in response to hyperoxia exposure. *Physiol Genomics* 44: 970–980, 2012.
- Biyashev D, Veliceasa D, Topczewski J, Topczewska JM, Mizgirev I, Vinokour E, Reddi AL, Licht JD, Revskoy Volpert OV. miR-27b controls venous specification and tip cell fate. *Blood* 119: 2679–2687, 2012.
- Bratinova-Kassova S, Yang G, Igarashi K, Dennery PA. Bach1 modulates heme oxygenase-1 expression in the neonatal mouse lung. *Pediatr Res* 65: 145–149, 2009.
- Buczynski BW, Madueke ET, O'Reilly MA. The role of hyperoxia in the pathogenesis of experimental BPD. *Semin Perinatol* 37: 69–78, 2013.
- Comer BS, Camoretti-Mercado B, Kogut PC, Halayko AJ, Solway J, Gerthoffer WT. MicroRNA-146a and microRNA-146b expression and anti-inflammatory function in human airway smooth muscle. *Am J Physiol Lung Cell Mol Physiol* 307: L727–L734, 2014.
- Croce CM. Causes and consequences of microRNA dysregulation in cancer. *Nat Rev Genet* 10: 704–714, 2009.
- Cushing L, Kuang PP, Qian J, Shao F, Wu J, Little F, Thannickal VJ, Cardoso WV, Lü J. miR-29 is a major regulator of genes associated with pulmonary fibrosis. *Am J Respir Cell Mol Biol* 45: 287–294, 2011.
- Dennery PA, Lee CS, Ford BS, Weng YH, Yang G, Rodgers PA. Developmental expression of heme oxygenase in the rat lung. *Pediatr Res* 53: 42–47, 2003.
- Dennery PA, Rodgers PA, Lum MA, Jennings BC, Shokoohi V. Hyperoxic regulation of lung heme oxygenase in neonatal rats. *Pediatr Res* 40: 815–821, 1996.
- Dong J, Carey WA, Abel S, Collura C, Jiang G, Tomaszek S, Sutor S, Roden AC, Asmann YW, Prakash YS, Wigle DA. MicroRNA-mRNA interactions in a murine model of hyperoxia-induced bronchopulmonary dysplasia. *BMC Genomics* 13: 204, 2012.
- Ehrenkranz RA, Walsh MC, Vohr BR, Jobe AH, Wright LL, Fanaroff AA, Wraage LA, Poole K. Validation of the National Institutes of Health consensus definition of bronchopulmonary dysplasia. *Pediatrics* 126: 443–456, 2005.
- Elton TS, Selemón G, Elton SM, Parinandi NL. Regulation of the MIR155 host gene in physiological and pathological processes. *Gene* 532: 1–12, 2013.
- Garbacki N, Di Valentin E, Huynh-Thu VA, Geurts P, Irrthum A, Crahay C, Arnould T, Deroanne C, Piette J, Cataldo D, Colige A. MicroRNAs profiling in murine models of acute and chronic asthma: a relationship with mRNAs targets. *PLoS One* 6: e16509, 2011.
- Harris KS, Zhang Z, McManus MT, Harfe BD, Sun X. Dicer function is essential for lung epithelium morphogenesis. *Proc Natl Acad Sci USA* 14: 2208–2213, 2006.
- Heegaard NH, Schetter AJ, Welsh JA, Yoneda M, Bowman ED, Harris CC. Circulating micro-RNA expression profiles in early stage nonsmall cell lung cancer. *Int J Cancer* 130: 1378–1387, 2012.
- Hou W, Tian Q, Steuerwald NM, Schrum LW, Bonkovsky HL. The let-7 microRNA enhances heme oxygenase-1 by suppressing Bach1 and attenuates oxidant injury in human hepatocytes. *Biochim Biophys Acta* 1819: 1113–1122, 2012.
- Hou W, Tian Q, Zheng J, Bonkovsky HL. MicroRNA-196 represses Bach1 protein and hepatitis C virus gene expression in human hepatoma cells expressing hepatitis C viral proteins. *Hepatology* 51: 1494–1504, 2010.
- Iliopoulos D, Hirsch HA, Struhl K. An epigenetic switch involving NF- $\kappa$ B, Lin28, Let-7 MicroRNA, and IL6 links inflammation to cell transformation. *Cell* 139: 693–706, 2009.
- Kurinna S, Werner S. NRF2 and microRNAs: new but awaited relations. *Biochem Soc Trans* 43: 595–601, 2015.
- Lee U, Frankenberger C, Yun J, Bevilacqua E, Caldas C, Chin SF, Rueda OM, Reinitz J, Rosner MR. A prognostic gene signature for metastasis-free survival of triple negative breast cancer patients. *PLoS One* 8: e82125, 2013.
- Liu G, Frigger A, Yang Y, Milosevic J, Ding Q, Thannickal VJ, Kaminski N, Abraham E. miR-21 mediates fibrogenic activation of pulmonary fibroblasts and lung fibrosis. *J Exp Med* 207: 1589–1597, 2010.
- Moschos SA, Williams AE, Perry MM, Birell MA, Belvisi MG, Lindsay MA. Expression profiling in vivo demonstrates rapid changes in lung microRNA levels following lipopolysaccharide-induced inflammation but not in the anti-inflammatory action of glucocorticoids. *BMC Genomics* 8: 240, 2007.
- Namba F, Go H, Murphy JA, La P, Yang G, Sengupta S, Fernando AP, Yohannes M, Biswas C, Wehrli SL, Dennery PA. Expression level and subcellular localization of heme oxygenase-1 modulates its cytoprotective properties in response to lung injury: a mouse model. *PLoS One* 9: e90936, 2014.
- Otterbein LE, Soares MP, Yamashita K, Bach FH. Heme oxygenase-1: unleashing the protective properties of heme. *Trends Immunol* 24: 449–455, 2003.
- Perry MM, Williams AE, Tsitsiou E, Larner-Svensson HM, Lindsay MA. Divergent intracellular pathways regulate interleukin-1 beta-induced miR-146a and miR-146b expression and chemokine release in human alveolar epithelial cells. *FEBS Lett* 583: 3349–3355, 2009.
- Song R, Liu Q, Hutvagner H, Ramamohanarao K, Wong L, Li J. Rule discovery and distance separation to detect reliable miRNA biomarkers for

- the diagnosis of lung squamous cell carcinoma. *BMC Genomics* 15, Suppl 9: S16, 2014.
33. Stefani G, Slack FJ. Small non-coding RNAs in animal development. *Nat Rev Mol Cell Biol* 9: 219–230, 2008.
  34. Sun J, Brand M, Zenke Y, Tashiro S, Groudine M, Igarashi K. Heme regulates the dynamic exchange of Bach1 and NF-E2-related factors in the Maf transcription factor network. *Proc Natl Acad Sci USA* 101: 1461–1466, 2004.
  35. Suttner DM, Dennery PA. Reversal of HO-1 related cytoprotection with increased expression is due to reactive iron. *FASEB J* 13: 1800–1809, 1999.
  36. Taganov KD, Boldin MP, Chang KJ, Baltimore D. NF-kappaB-dependent induction of microRNA miR-146, an inhibitor targeted to signaling proteins of innate immune responses. *Proc Natl Acad Sci USA* 103: 12481–12486, 2006.
  37. Van Marter LJ, Kuban KC, Allred E, Bose C, Dammann O, O'Shea M, Laughon M, Ehrenkranz RA, Schreiber MD, Karna P, Leviton A; ELGAN Study Investigators. Does bronchopulmonary dysplasia contribute to the occurrence of cerebral palsy among infants born before 28 weeks of gestation? *Arch Dis Child Fetal Neonatal Ed* 96: F20–F29, 2011.
  38. Vaporidi K, Vergadi E, Kaniaris E, Hatziaepostolou M, Lagoudaki E, Georgopoulos D, Zapol WM, Bloch KD, Iliopoulos D. Pulmonary microRNA profiling in a mouse model of ventilator-induced lung injury. *Am J Physiol Lung Cell Mol Physiol* 303: L199–L207, 2012.
  39. Wakabayashi N, Skoko JJ, Chartoumpekis DV, Kimura S, Slocum SL, Noda K, Palliyaguru DL, Fujimuro M, Boley PA, Tanaka Y, Shigemura N, Biswal S, Yamamoto M, Kensler TW. Notch-Nrf2 axis: regulation of Nrf2 gene expression and cytoprotection by notch signaling. *Mol Cell Biol* 34: 653–663, 2014.
  40. Wang Y, Stricker HM, Gou D, Liu L. MicroRNA: past and present. *Front Biosci* 12: 2316–2329, 2007.
  41. Wang Y, Weng T, Gou D, Chen Z, Chintagari NR, Lui L. Identification of rat lung-specific microRNAs by microRNA microarray: valuable discoveries for facilitation of lung research. *BMC Genomics* 8: 29, 2007.
  42. Wei R, Huang GL, Zhang MY, Li BK, Zhang HZ, Shi M, Chen XQ, Huang L, Zhou QM, Jia WH, Zheng XF, Yuan YF, Wang HY. Clinical significance and prognostic value of microRNA expression signatures in hepatocellular carcinoma. *Clin Cancer Res* 19: 4780–4791, 2013.
  43. Williams AE, Moschos SA, Perry MM, Barnes PJ, Lindsay MA. Maternally imprinted microRNAs are differentially expressed during mouse and human lung development. *Dev Dyn* 236: 572–580, 2007.
  44. Williams AE, Perry MM, Moschos SA, Lindsay MA. MicroRNA expression in the aging mouse lung. *BMC Genomics* 8: 172, 2007.
  45. Yang S, Banerjee S, de Freitas A, Sanders YY, Ding Q, Matalon S, Thannickal VJ, Adraham E, Liu G. Participation of miR-200 in pulmonary fibrosis. *Am J Pathol* 180: 484–493, 2012.
  46. Zhang W, Feng JQ, Harris SE, Contag PR, Stevenson DK, Contag CH. Rapid in vivo functional analysis of transgenes in mice using whole body imaging of luciferase expression. *Transgenic Res* 10: 423–434, 2001.

